

Room temperature homogeneous flow in a bulk metallic glass with low glass transition temperature

K. Zhao, X. X. Xia, H. Y. Bai, D. Q. Zhao, and W. H. Wang^{a)}

Institute of Physics, Chinese Academy of Sciences, Beijing 100190, People's Republic of China

(Received 12 February 2011; accepted 17 March 2011; published online 7 April 2011)

We report a high entropy metallic glass of $\text{Zn}_{20}\text{Ca}_{20}\text{Sr}_{20}\text{Yb}_{20}(\text{Li}_{0.55}\text{Mg}_{0.45})_{20}$ via composition design that exhibiting remarkable homogeneous deformation without shear banding under stress at room temperature. The glass also shows properties such as low glass transition temperature (323 K) approaching room temperature, low density and high specific strength, good conductivity, polymerlike thermoplastic manufacturability, and ultralow elastic moduli comparable to that of bones. The alloy is thermally and chemically stable. © 2011 American Institute of Physics. [doi:10.1063/1.3575562]

The bulk metallic glasses (BMGs) suffer a strong drawback of shear localization and macroscopically brittle failure at ambient temperature. The room temperature (RT) plastic deformation of BMGs is highly inhomogeneous and is localized in the thin shear bands. The brittleness is regarded as an intrinsic defect of the metallic glasses.¹ Extensive efforts have been made to improve their limited plasticity at RT.²⁻⁴ Generally speaking, there are two categories of methods to enhance the plasticity of BMGs: (i) the reduction in sample size and (ii) the introduction of heterogeneity. Ductility has been shown to increase dramatically at small length scales.^{2,4} By introducing structural heterogeneities, the compressive plasticity of BMGs can also be markedly improved.³ However, on bulk scale, the large homogeneous deformation without shear banding at RT in the BMGs has never been reported so far.

The plastic deformation behavior in a glass is related to the strain rate and the ratio of test temperature (T_t) to glass transition temperature (T_g), $T_r (=T_t/T_g)$.¹ Theoretically, the homogeneous flow of metallic glasses could take place below T_g at extreme low strain rates or high T_r (>0.85).⁵ It is expected that the decrease in T_g of a BMG, which corresponds to increase in T_r ($T_r = T_t/T_g = \text{RT}/T_g$), could be another route for improving the plasticity of the BMGs at RT. Recently, some BMGs (such as Ce-, Au-, Sr-, and Yb-based BMGs) with low T_g has been developed.⁶⁻¹⁰ While the Sr-based BMGs with very low T_g and high T_r (>0.90) have very poor corrosion resistance and are usually highly unstable,^{6,9} and the deformation at RT for Ce-, Yb-, and Au-based BMGs was found to be inhomogeneous.⁶⁻¹¹

In this letter, we report the formation of a BMG by composition design. Properties studies show that the BMG, consisting of the cheaper main components, offers combining excellent physical properties. Especially, it exhibits homogeneous deformation at RT, which presents direct evidence to demonstrate that BMGs could be deformed homogeneously at RT.

To increase the T_r for the alloy, we attempt to decrease its T_g . Actually, many desirable and combining properties of a BMG can be attributed to its ultralow T_g .⁷ The sufficient

data exhibit that the T_g and elastic moduli of BMGs are clearly correlated.¹² The lower elastic moduli gives lower T_g , and elastic constants of BMGs show a correlation with a weighted average of the elastic constants for the constituent elements. The established elastic moduli and T_g correlation is our guidelines for development of BMG with low T_g by appropriate composition selection of components. The Li, Ca, Sr, Yb, and Mg were chosen due to their low elastic modulus.¹² While all the Ca, Sr, Li, and Mg are active elements, we then chosen Zn, which has been proved to be effective for improving the corrosion resistance of BMGs.¹³ According to confusion principle,¹⁴ the more elements involved, the higher possibility for the alloy to have higher glass-forming ability. The high mixing entropy is another route for design new alloys.¹⁵ Following above criteria and ideas, we chosen six components with similar fraction in the alloy to increase the mixing entropy and improve glass-forming ability. By melting $\text{Li}_{55}\text{Mg}_{45}$ master alloy with Ca (99%), Sr (99%), Zn (99.9%), and Yb (99%) elements using induction-melting method in a quartz tube under vacuum (better than 3.0×10^{-3} Pa) and subsequently casting into copper mold, a multi-component BMG with a nominal composition of $\text{Zn}_{20}\text{Ca}_{20}\text{Sr}_{20}\text{Yb}_{20}(\text{Li}_{0.55}\text{Mg}_{0.45})_{20}$ is obtained in cylindrical shape (diameter ≥ 3 mm) or in plate forms or in other complex shapes with shiny metallic surfaces like other BMGs based on Zr, Cu, and Fe.

The amorphicity throughout the thickness of the as-cast and deformed samples was examined by x-ray diffraction (XRD) using a MAC M03 diffractometer (Cu K_α radiation) as shown in Fig. 1(a). The broad diffraction peaks without appreciable sharp crystalline peaks in the XRD curve indicate that the alloy can be easily cast into bulk glasses. Figure 1(b) shows the differential scanning calorimetry (DSC) trace (performed under a purified argon atmosphere in a Mettler Toledo DSC822e with a heating rate of 20 K/min.), and the inset is its DSC trace of melting. The sample has distinct glass transition and sharp crystallization peaks in its DSC trace, which confirms the glassy structure. The crystallization temperature T_x , liquidus temperature T_l , and the supercooled liquid region ($\Delta T = T_x - T_g$) and reduced glass transition temperature ($T_{rg} = T_g/T_l$) of the alloy are 348 K, 561 K, 25 K, and 0.58 K, respectively. The designed BMG indeed has ultralow T_g (~ 323 K) and approaches RT. The value of T_g is

^{a)} Author to whom correspondence should be addressed. Electronic mail: whw@aphy.iphy.ac.cn.

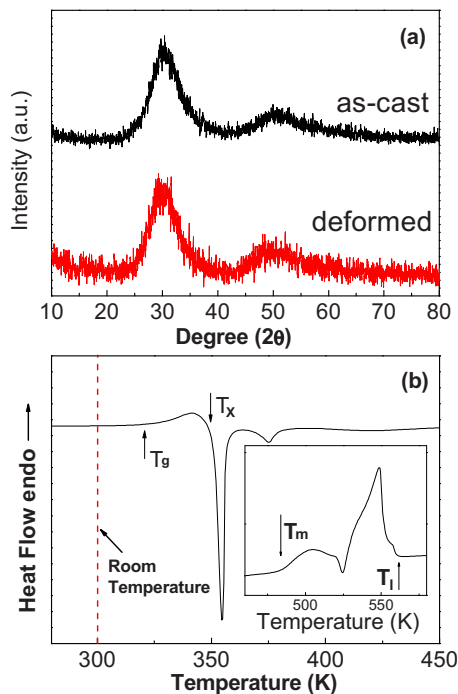


FIG. 1. (Color online) (a) XRD patterns of $\text{Zn}_{20}\text{Ca}_{20}\text{Sr}_{20}\text{Yb}_{20}(\text{Li}_{0.55}\text{Mg}_{0.45})_{20}$ in as-cast state and after 70% plastic deformation. (b) DSC traces of as-cast $\text{Zn}_{20}\text{Ca}_{20}\text{Sr}_{20}\text{Yb}_{20}(\text{Li}_{0.55}\text{Mg}_{0.45})_{20}$.

similar to or even lower than that of some amorphous polymers.

Compression tests at RT were performed on a series of BMGs with gauge aspect ratio of 2:1 cut out of the as-cast 2 mm rod. The markedly different values of T_g for $\text{Fe}_{64}\text{Mo}_{14}\text{C}_{15}\text{B}_6\text{Er}_1$, $\text{Zr}_{41}\text{Ti}_{14}\text{Cu}_{12.5}\text{Ni}_{10}\text{Be}_{22.5}$, $\text{Mg}_{65}\text{Cu}_{25}\text{Y}_9\text{Gd}_1$, $\text{Pr}_{60}\text{Al}_{10}\text{Ni}_{10}\text{Cu}_{20}$, $\text{Ce}_{62}\text{Al}_{10}\text{Cu}_{20}\text{Co}_3\text{Ni}_5$, and $\text{Zn}_{20}\text{Ca}_{20}\text{Sr}_{20}\text{Yb}_{20}(\text{Li}_{0.55}\text{Mg}_{0.45})_{20}$ BMGs are 783 K, 623 K, 423 K, 409 K, 367 K, and 323 K, respectively. And their values of $T_r = \text{RT}/T_g$ are 0.38, 0.48, 0.71, 0.73, 0.82, and 0.93, respectively. Figure 2(a) shows the stress-strain curves at RT of those BMGs. The BMGs with high T_g exhibit elastic strain limit of $\sim 2\%$ followed by catastrophic failure. While for $\text{Zn}_{20}\text{Ca}_{20}\text{Sr}_{20}\text{Yb}_{20}(\text{Li}_{0.55}\text{Mg}_{0.45})_{20}$ BMG, after elastic strain limit of $\sim 2\%$ (the yield strength σ_Y is about 400 MPa), it remarkably displays stress overshoot as is often observed in homogeneous deformation in the supercooled liquid state (e.g., for Zr- and Pd-based BMGs, the homogeneous deformation occurs in temperature high than 500 K),¹⁷ and the stress overshoot is generally thought to be caused by the change in free volume during deformation. After the overshoot, the stress σ attains a steady state [see Fig. 2(b)] which is a typical feature of the homogeneous flow. As shown in the picture of Fig. 2(c), the sample can be compressed to 70% of its original height without observable cracking and shear banding, and further compression is still possible to extend the deformation. When the strain rate decreases to 10^{-5} s^{-1} , the yielding stress and steady flow stress decrease [Fig. 2(b)]. Such a heavily deformation without shear bands and fracture and the strain rate dependence of the steady state flow stress indicates the homogeneous flowability of the BMG at RT. Previously, such exceptional deformability and flexibility can only be obtained in supercooled liquid state at high temperatures and has never been observed at RT for conventional BMGs, which would fail after little observable plastic strain. The XRD [Fig. 1(a)] ex-

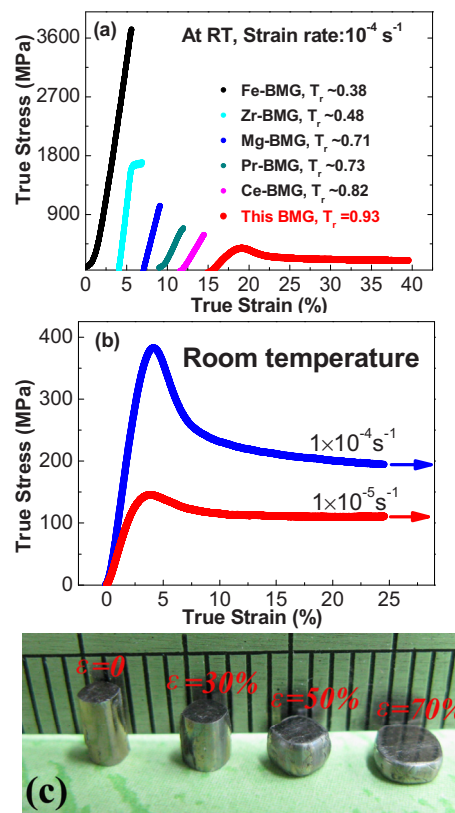


FIG. 2. (Color online) (a) Stress-Strain curves of the $\text{Zn}_{20}\text{Ca}_{20}\text{Sr}_{20}\text{Yb}_{20}(\text{Li}_{0.55}\text{Mg}_{0.45})_{20}$ ($T_g = 323 \text{ K}$) and $\text{Fe}_{64}\text{Mo}_{14}\text{C}_{15}\text{B}_6\text{Er}_1$ ($T_g = 783 \text{ K}$), $\text{Zr}_{41}\text{Ti}_{14}\text{Cu}_{12.5}\text{Ni}_{10}\text{Be}_{22.5}$ ($T_g = 623 \text{ K}$), $\text{Mg}_{65}\text{Cu}_{25}\text{Y}_9\text{Gd}_1$ ($T_g = 423 \text{ K}$), $\text{Pr}_{60}\text{Al}_{10}\text{Ni}_{10}\text{Cu}_{20}$ ($T_g = 409 \text{ K}$), and $\text{Ce}_{62}\text{Al}_{10}\text{Cu}_{20}\text{Co}_3\text{Ni}_5$ ($T_g = 367 \text{ K}$) samples. (b) Highlight the stress-strain curves for the $\text{Zn}_{20}\text{Ca}_{20}\text{Sr}_{20}\text{Yb}_{20}(\text{Li}_{0.55}\text{Mg}_{0.45})_{20}$ at strain rates of 10^{-4} and 10^{-5} s^{-1} . (c) The photo image of the compressed samples. They could be compressed to 70% of its original height without shear banding and cracking.

amination verifies that the severely deformed samples remain fully amorphous.

Figure 3(a) shows the scanning electron microscopy (SEM) image of the compressed $\text{Zn}_{20}\text{Ca}_{20}\text{Sr}_{20}\text{Yb}_{20}(\text{Li}_{0.55}\text{Mg}_{0.45})_{20}$ sample with a strain $\epsilon \approx 25\%$. Figure 3(b) shows the enlarged SEM image of the sample. The severely deformed specimen almost keeps the

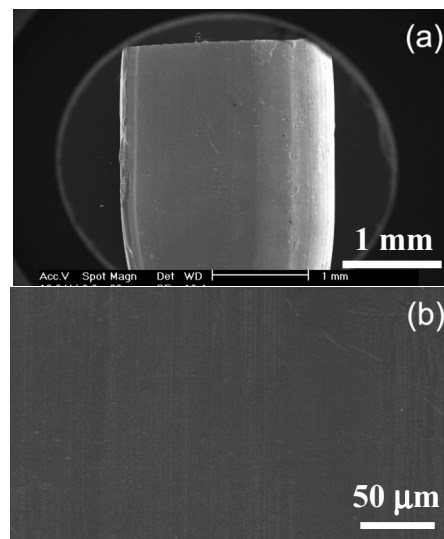


FIG. 3. Macroscopic (a) and microscopic (b) SEM image of the 25% deformed $\text{Zn}_{20}\text{Ca}_{20}\text{Sr}_{20}\text{Yb}_{20}(\text{Li}_{0.55}\text{Mg}_{0.45})_{20}$ BMG.

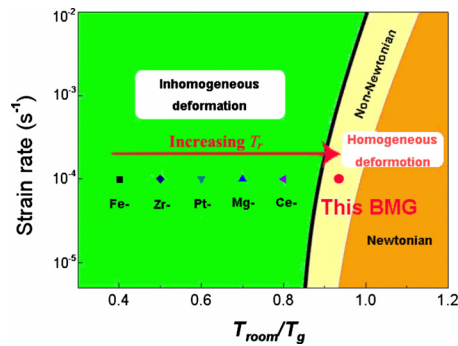


FIG. 4. (Color online) The location of BMGs with different glass transition temperatures and deformation behaviors in deformation map for metallic glasses in strain rate—temperature axes. The $\text{Zn}_{20}\text{Ca}_{20}\text{Sr}_{20}\text{Yb}_{20}(\text{Li}_{0.55}\text{Mg}_{0.45})_{20}$ BMGs locates in homogeneous deformation due to its high value of T_r at RT.

smooth surface of the as-cast state and no primary shear bands and other observable shear bands can be found. This confirms the uniform deformation and the homogeneous flow occurs in the metallic glass at RT, which may alter the conventional wisdom on metallic glasses which were regarded to be intrinsically brittle.

For conventional BMGs, such as Fe-, Zr-, Pt-, Mg-, and Ce-based ones, their value of T_r at RT ranges between 0.4 and 0.8, and locates in the inhomogeneous region in quasi-static compression test as indicated in the deformation map¹ shown in Fig. 4. When T_r reaches 0.85, it is expected that the deformation of the glass changes from localized and inhomogeneous state to homogeneous state, and homogeneous flow would occur at RT.¹ The origin of the homogeneous flow and the extreme deformability of the BMG is realized by markedly increase the value of T_r via modification of its T_g using the elastic moduli empirical criteria.¹² The obtained BMG indeed has low elastic moduli, and the Young's modulus E , shear modulus G , bulk modulus B , and Poisson ratio ν measured by ultrasonic method at RT using a pulse echo overlap method [with a carry frequency of 10 MHz (Ref. 12)] are 16 GPa, 6.3 GPa, 12 GPa, and 0.28 GPa, respectively. Figure 5 shows the comparisons of E and G between $\text{Zn}_{20}\text{Ca}_{20}\text{Sr}_{20}\text{Yb}_{20}(\text{Li}_{0.55}\text{Mg}_{0.45})_{20}$ and other BMGs. It shows clearly that the elastic constants of $\text{Zn}_{20}\text{Ca}_{20}\text{Sr}_{20}\text{Yb}_{20}(\text{Li}_{0.55}\text{Mg}_{0.45})_{20}$ are the lowest in known BMGs so far. Such ultralow elastic moduli make the BMG have ultralow value of T_g (323 K), and then its $T_r = \text{RT}/T_g$ reaches a high value of 0.93 at RT, which makes it stand in the homogeneous deformation region, which is consistent with the experimental results of our compression test.

The flow barrier energy W_{STZ} of shear transformation zones (STZs) in metallic glasses can be estimated by $W_{\text{STZ}} \propto GV_m$,¹⁷ where V_m is average molar volume. The BMGs with lower W_{STZ} have good ductility. Due to the ultralow G (6.3 GPa), the BMG has much lower activation energy for the STZs compared with that of other known BMGs, the activation of STZs is then much easier, which leads to homogeneous deformation of the glass. The decrease in T_g or G is another route for the design of ductile metallic glasses.

Our BMG with ultralow T_g makes the BMG show polymerlike thermoplastic formability near RT. It can be repeatedly compressed, stretched, bent, and formed into complicated shapes even nanoimprinted patterns demonstrating the excellent thermoplastic processability as the conventional

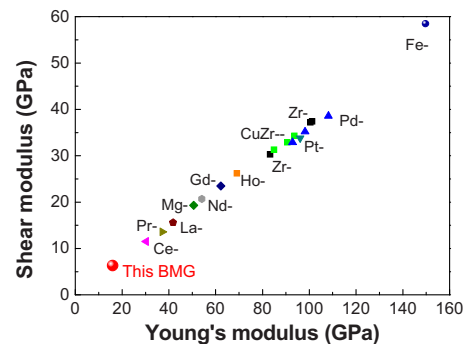


FIG. 5. (Color online) The Young's modulus and shear modulus of a series BMGs (Ref. 12) The $\text{Zn}_{20}\text{Ca}_{20}\text{Sr}_{20}\text{Yb}_{20}(\text{Li}_{0.55}\text{Mg}_{0.45})_{20}$ BMG has the smallest elastic constant among other typical BMGs.

polymeric materials.⁷⁻⁹ The electrical resistivity of BMG is $140 \mu\Omega \text{ cm}$ which is similar to manganese's. The BMG has much better oxidation resistance than that of other BMGs (such as Sr-, Ca-, and Ce-based BMGs) with low T_g . In ambient conditions the BMG has bright silvery surface. The density ρ of the BMG, and hardness are determined to be 3.6 g/cm^3 and 0.82 GPa, respectively, and are much lower than compared to that of conventional BMGs.

The metallic glasses are often called as “liquid metals,” the finding of the viscoplastic BMG makes the term of liquid metals a reality due to the significant viscoplastic flow at RT. The apparent viscosity of the BMG at RT can be estimated by $\eta_a = (\sigma/3\dot{\epsilon})$, where σ is the normal stress and $\dot{\epsilon}$ is the strain rate. At $\dot{\epsilon} = 10^{-4} \text{ s}^{-1}$, the steady state flow stress σ is about 200 MPa, and the apparent viscosity η_a of the BMG is about 10^{12} Pa s , which is close to the viscosity of super-cooled liquid state near T_g .^{1,12} The alloy indeed stands at the boundary between the solid and liquid.

Financial support is from NSF of China (Grant Nos. 50921091 and 50731008) and MOST973 of China (Grant Nos. 2007CB613904 and 2010CB731603).

¹C. A. Schuh, T. C. Hufnagel, and U. Ramamurty, *Acta Mater.* **55**, 4067 (2007).

²H. A. Atwater and A. Polman, *Nature Mater.* **9**, 205 (2010).

³Y. H. Liu, G. Wang, R. J. Wang, M. X. Pan, and W. H. Wang, *Science* **315**, 1385 (2007).

⁴H. Guo, P. F. Yan, J. Tan, Z. F. Zhang, M. L. Sui, and E. Ma, *Nature Mater.* **6**, 735 (2007).

⁵M. L. Falk and J. S. Langer, *Phys. Rev. E* **57**, 7192 (1998).

⁶K. Zhao, J. F. Li, D. Q. Zhao, and W. H. Wang, *Scr. Mater.* **61**, 1091 (2009).

⁷B. Zhang, D. Q. Zhao, W. H. Wang, and A. L. Greer, *Phys. Rev. Lett.* **94**, 205502 (2005).

⁸W. Zhang, H. Guo, M. W. Chen, Y. Saotome, and A. Inoue, *Scr. Mater.* **61**, 744 (2009).

⁹J. F. Li, D. Q. Zhao, M. L. Zhang, and W. H. Wang, *Appl. Phys. Lett.* **93**, 171907 (2008).

¹⁰J. Q. Wang, W. H. Wang, and H. Y. Bai, *Appl. Phys. Lett.* **94**, 041910 (2009).

¹¹B. Yang, J. Wadsworth, and T. G. Nieh, *Appl. Phys. Lett.* **90**, 061911 (2007).

¹²W. H. Wang, *J. Appl. Phys.* **99**, 093506 (2006).

¹³B. Zberg, P. J. Uggowitzer, and J. F. Löffler, *Nature Mater.* **8**, 887 (2009).

¹⁴A. L. Greer, *Nature (London)* **366**, 303 (1993).

¹⁵C. J. Tong, Y. L. Chen, S. K. Chen, J. W. Yeh, and S. Y. Chang, *Mater. Trans. A* **36A**, 882 (2005).

¹⁶H. Kato, Y. Kawamura, A. Inoue, and H. S. Chen, *Appl. Phys. Lett.* **73**, 3665 (1998).

¹⁷H. B. Yu, W. H. Wang, H. Y. Bai, Y. Wu, and M. W. Chen, *Phys. Rev. B* **81**, 220201(R) (2010).